

Evolution of Correlated Electrons in $\text{La}_3\text{Ni}_2\text{O}_7$ at Ambient Pressure: a Study of Double-Counting Effect

Zhong-Yi Xie¹, Zhihui Luo¹, Wéi Wú¹, and Dao-Xin Yao^{1*}

¹Guangdong Provincial Key Laboratory of Magnetoelectric Physics and Devices, State Key Laboratory of Optoelectronic Materials and Technologies, Center for Neutron Science and Technology, School of Physics, Sun Yat-sen University, Guangzhou, Guangdong 510275, China.

*Corresponding author(s). E-mail(s): yaodaox@mail.sysu.edu.cn;
Contributing authors: xiezy9@mail2.sysu.edu.cn;
luozhh59@mail.sysu.edu.cn; wuwei69@mail.sysu.edu.cn;

Abstract

We employ cluster extension of dynamical mean-field theory (CDMFT) to systematically investigate the impact of double counting corrections on the correlated electronic structure of $\text{La}_3\text{Ni}_2\text{O}_7$ under ambient pressure. By adjusting double-counting parameters, while maintaining a fixed Fermi surface, we observe a pronounced orbital-selective density of states change: the d_{z^2} orbital undergoes significant variation near the Fermi level with increasing E_{dc}^z , while the $d_{x^2-y^2}$ orbital remains essentially unchanged throughout the entire range. Analysis of renormalization factor show the monotonic dependence with double counting in both d_{z^2} and $d_{x^2-y^2}$ orbital, and it also identifies an optimal double counting window in d_{z^2} orbital aligns with experimental values. We also find the interlayer Matsubara self energy exhibits non-monotonic dependence on E_{dc}^z , deviating from theoretical predictions. This anomaly is attributed to the metallization of oxygen-bridged pathways, which disrupts the prerequisite for charge transfer via apical oxygen. Our results establish E_{dc} as a critical control parameter for correlated electronic structure in $\text{La}_3\text{Ni}_2\text{O}_7$ and provide a computational framework for resolving orbital-dependent correlation effects in layered materials.

Keywords: CDMFT, $\text{La}_3\text{Ni}_2\text{O}_7$, double counting effect

1 Introduction

The dynamical mean-field theory (DMFT) has emerged as an established methodology for calculating the electronic structure of strongly correlated materials, with recent advancements demonstrating its effectiveness in resolving complex many-body interactions that traditional density functional theory (DFT) approximations fail to capture[1–3]. However, an underlying problem of this approach comes from the estimation of the double-counting energy (E_{dc}), which is designated to remove the equivalent contribution within the correlated subspace that is already accounted for at the DFT level. This issue appears when the system contains both correlated and uncorrelated electrons. A common example would be the transition metal compounds, where the charge transfer energy (E_{CT}) between the correlated ions and its ligands becomes the characteristic energy scale[4]. Here the choice of E_{dc} will directly affect E_{CT} , which is even pronounced in the charge-transfer limit $E_{CT} \rightarrow 0$. Several double-counting choices have been proposed [5–7] but an exact prescription is unattainable for the general cases.

Recently, transition temperature (T_c) reaching ~ 80 K under high pressure was found in the bilayer nickelate $\text{La}_3\text{Ni}_2\text{O}_7$ [8]. The average valence state of nickel (Ni) atoms in $\text{La}_3\text{Ni}_2\text{O}_7$ is $\text{Ni}^{2.5+}$ ($3d^{7.5}$), which contains the fully-filled t_{2g} and partial filling of e_g orbitals. The fundamental building block of $\text{La}_3\text{Ni}_2\text{O}_7$ consists of two quasi-two-dimensional NiO_2 planes, which are coupled via σ -bonding of d_{z^2} mediated by apical O- $2p_z$ orbital. The half-filling of d_{z^2} orbital suggests an effective interlayer superexchange coupling that is believed to be crucial for the superconductivity[9]. The superexchange coupling is regulated by the hopping d_{z^2} - p [10] with the cost of the energy difference Δ_{dp} . Therefore, a careful choice of the E_{dc} would be important to correctly account for the superconducting properties.

In this paper, we systematically investigate the impact of double counting energy on the correlated electronic structure for $\text{La}_3\text{Ni}_2\text{O}_7$ under ambient pressure. A charge-transfer 11 orbital model of $\text{La}_3\text{Ni}_2\text{O}_7$ that contains 4 Ni-d orbitals (2 Ni atoms with two orbitals $d_{x^2-y^2}$, d_{z^2} per Ni) and 7 ligand oxygen p orbitals is used, which is solved self-consistently under CDMFT. To ensure physical validity, besides explicitly adjusting the E_{dc} values in a plausible range, we also rigorously compare the calculated Fermi surface (FS) profile to match that from the experimentally angle-resolved photoemission spectroscopy (ARPES)[11]. With this, we investigate the evolution of electron density, density of states (DOS) and non-local interlayer correlation to gain a comprehensive understanding of the correlation feature. Also, a comparison to two commonly used double-counting schemes, the fully localized limit (FLL)[7] and Held formulas[12], are presented.

2 Model and Method

We consider an 11-band Hubbard model that can be written as:

$$H = H_0 + H_U - \sum_{i,\alpha,\sigma} E_{dc}^\alpha n_{i\alpha\sigma}^d \quad (1)$$

$$H_0 = \sum_{i,j,\alpha,\beta,\sigma} t_{i,j,\alpha,\beta} d_{i\alpha\sigma}^\dagger p_{j\beta\sigma} + \sum_{i,j,\alpha,\beta,\sigma} t_{i,j,\alpha,\beta} p_{i\alpha\sigma}^\dagger p_{j\beta\sigma} - \sum_{i,\alpha,\sigma} \mu_\alpha n_{i\alpha\sigma} \quad (2)$$

$$H_U = U \sum_{i,\alpha} n_{i\alpha\uparrow}^d n_{i\alpha\downarrow}^d + U' \sum_{i,\alpha<\beta,\sigma} n_{i\alpha\sigma}^d n_{i\beta\sigma}^d + (U' - J_H) \sum_{i,\alpha<\beta,\sigma} n_{i\alpha\sigma}^d n_{i\beta\sigma}^d + J_H \sum_{i,\alpha\neq\beta} (d_{i\alpha\uparrow}^\dagger d_{i\alpha\downarrow}^\dagger d_{i\beta\uparrow} d_{i\beta\downarrow} - d_{i\alpha\uparrow}^\dagger d_{i\alpha\downarrow} d_{i\beta\downarrow}^\dagger d_{i\beta\uparrow}) \quad (3)$$

Here H_0 is the tight-binding Hamiltonian determined out of our DFT calculation which implemented in the Vienna ab initio simulation package (VASP)[13, 14]. The projector augmented-wave (PAW) method[15] with a 600 eV plane-wave cut-off is adopted. The generalized gradient approximation (GGA) of Perdew-Burke-Ernzerhof (PBE)[16] is used for exchange-correlation functional. $t_{i,j,\alpha,\beta}$ denote hoppings between electrons on sites (i, j) and orbital (α, β) (can be either Ni-d or O-p orbitals). $d_{\alpha,i,\sigma}^\dagger (p_{\alpha,i,\sigma}^\dagger)$ is the creation operator for electrons on $\alpha \in 3d(\in 2p)$ orbital. μ is the chemical potential of α -orbital. The schematic diagram of this model can be referred to in [17], and the basis is defined as: $\Phi = (d_{z_1}, d_{z_2}, d_{x_1}, d_{x_2}, p_{x_1}, p_{x_2}, p_{y_1}, p_{y_2}, p_z, p'_{z_1}, p'_{z_2})^T$. 1,2 label the bilayer, d_z, d_x label $d_{z^2}, d_{x^2-y^2}$ orbitals, p_x and p_y label the in-plane O's p-orbital, p_z labels the inner apical O's p-orbital and p'_z labels outer apical O's p-orbital. H_U is the Kanamori Coulomb interaction term, U is the Hubbard interaction between two electrons on the same d-orbital ($d_{x^2-y^2}$ or d_{z^2}) and U' is for that on two different d-orbitals. $U' = U - 2J_H$ is adopted, where J_H is the Hund's coupling, and intensity of spin flip term is same as pair hopping term. E_{dc} is the double counting term to be subtracted in the DMFT.

We solve the lattice model within the framework of DMFT. DMFT is a powerful non-perturbative approach that maps a lattice problem onto an effective Anderson single-impurity model, which is then solved self-consistently[18–20]. This mapping becomes exact in the limit of infinite dimensions but it is also precise enough in two-dimensional system, and neglects all nonlocal contributions to the retarded self-energy. So the retarded self energy and Green's function is purely local, i.e., $\Sigma_{imp}(\omega) = \Sigma(\omega)$; $G_{imp}(\omega) = G_{loc}(\omega) = \frac{1}{N_k} \sum_k G(k, \omega)$. Furthermore, we employed CDMFT to incorporate non-local interactions between layers[21–23], which captures the interlayer correlation properties in $\text{La}_3\text{Ni}_2\text{O}_7$ materials. Specifically, four orbitals ($d_{z_1}, d_{z_2}, d_{x_1}, d_{x_2}$) are explicitly treated to form the cluster basis because of their predominance around the Fermi surface, while the electrons from remaining orbitals are encapsulated through a hybridization function that mediates their interactions with the impurity electrons.

In our CDMFT study, we use $U = 8$ eV and $J_H = 1$ eV to calculate an effective impurity model with the $2 \times 2 = 4$ orbitals which could introduce nonlocal interlayer coupling under $\beta = 25$. We use quantum Monte Carlo as the impurity solver, its number of steps is set to 10000 and length of step is set to 10000 which keeps the correction time ~ 1 s. Here, we use the open-source TRIQS[24] package and its continuous-time quantum Monte Carlo[25] for CDMFT and its impurity solver, respectively.

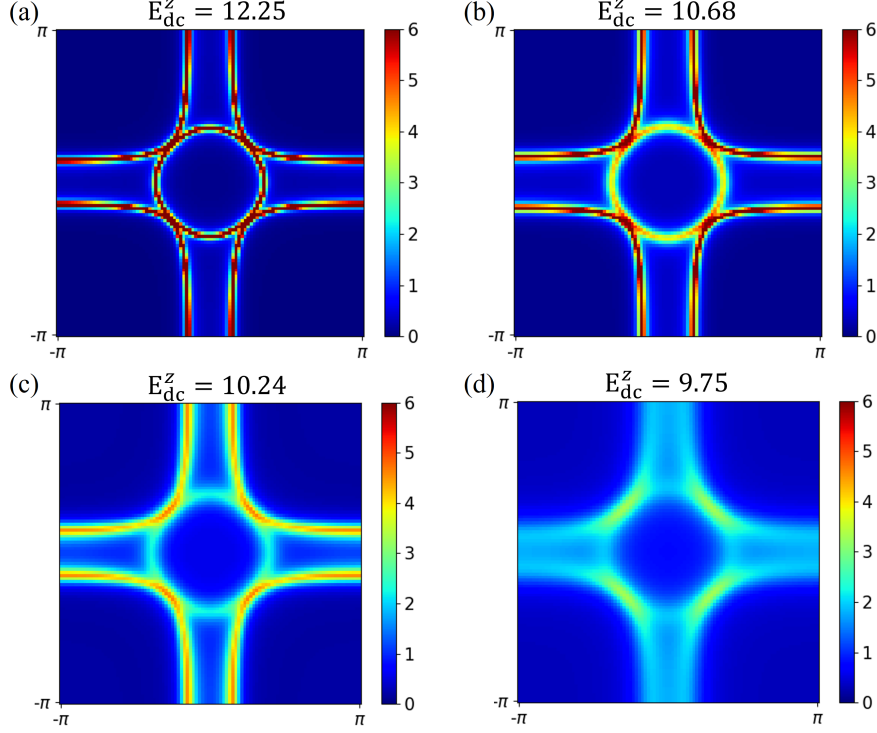


Fig. 1 The evolution of Fermi surface with decreasing the double-counting energies E_{dc}^z . Here the Fermi surface profile is manually adjusted to match that from the ARPES result[11], which leads to only one independent parameter among $(E_{dc}^z, E_{dc}^x, \mu_{pz})$, see main text for details.

Given that there are two types of inequivalence correlated orbitals in the model, a consideration of the orbital-dependent double-counting energy for both E_{dc}^x, E_{dc}^z would be more reasonable for the real situation but on the other hand bring an expansion of the adjustable parameter range. To simplify the consideration, we carefully align our DMFT Fermi surface profile with that from the ARPES for each tuning. We find this procedure makes E_{dc}^x and E_{dc}^z depend on each other, but on the other hand, the site energy of apical p_z orbital has to vary as well. That means for each tuning, the fitting of FS can determine a set of parameters $(E_{dc}^z, E_{dc}^x, \mu_{pz})$. Therefore, in the following, we only present the relevant physical quantities as a function of E_{dc}^z .

3 Results

We first demonstrate the Fermi surface as a function of E_{dc}^z , as shown in Fig. 1. One can see that only two pockets α, β show up, with each profile and position in precise agreement with the ARPES result[11] under ambient pressure. The major difference comes from the coherence. When E_{dc}^z is large, as shown in Fig. 1(a), there is well-defined quasiparticle dispersion of both pockets, indicating Fermi liquid behavior. As

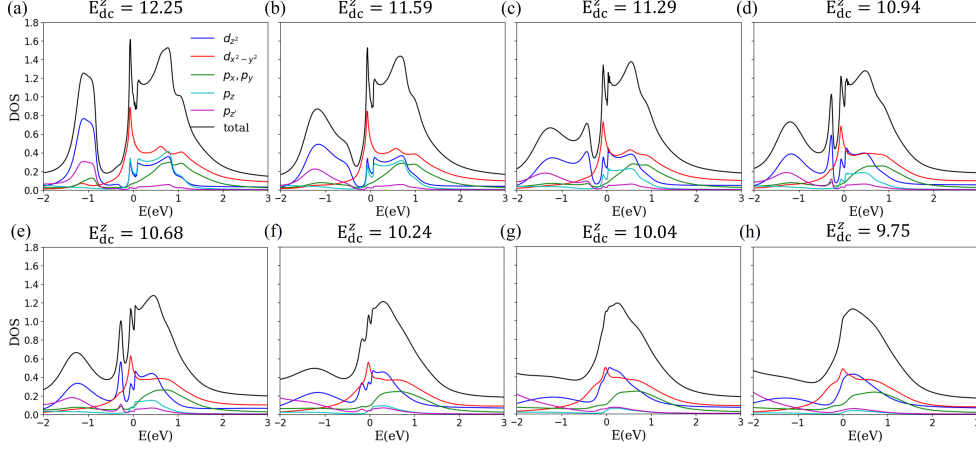


Fig. 2 Evolution of DOS as a function of E_{dc}^z .

decreasing E_{dc}^z , the incoherence is gradually enhanced, followed by the broadening of the spectrum, which is even pronounced in Fig. 1(d).

To better understand the above features, we next present the evolution of density of states (DOS) around Fermi energy (E_F) as a function of E_{dc}^z , as shown in Fig. 2. In Fig. 2(a), which corresponds to that in Fig. 1(a), the DOS exhibits two major branches: one centers around -1 eV and the other spans around 0-2 eV, and they are separated by a gap of ~ 0.8 eV. Orbital-resolved DOS further reveals that the low energy branch is mostly associated with a mixing of d_{z^2} orbital with apical O- p_z orbital that outside the bilayer, while the other branch contains complex mixing of all orbitals. Moreover, a notable dip is observed precisely at E_F , which is shaped by a sharp tip beneath E_F from $d_{x^2-y^2}$ orbital, and an above one from the antibonding band of d_{z^2} orbital. As decreasing E_{dc}^z , the low-energy branch is broadened and then shows a signal of splitting at $E_{dc}^z=11.29$ (Fig. 2(c)). Further decreasing E_{dc}^z leads the upper splitted band to merge into the high-energy branch. Eventually, all fine features are invisible with only one plain peak characterizes the spectrum, as illustrated in Fig. 2(f-h). No doubt that E_{dc}^z in this range is too far away from the real material. However, even in the physical plausible range from Fig. 2(a)-(e), there is drastic evolution of DOS with E_{dc}^z only spans ~ 1.5 eV. This highlights a sensitive dependence of the correlation feature on the double-counting energies.

The tip at E_F persists from Fig. 2(a)-(e) indicates an intrinsic connection to the FS topology. To gain insight, we further inspect $A(k, E)$ spectrum, which reveals that the sharp tip beneath E_F is mostly associated with the nearly flat band around Γ -X path (no shown), which can further track back to the proximity of β pocket to the X ($\pi, 0$) point, as shown in Fig. 1. It is interesting to note that, both ARPES and tunneling experiments[26] reveal the presence of a gap at E_F that is in line with our calculation.

Fig. 3(a) displays the electron density evolution of d-orbital states as a function of E_{dc}^z . The analysis reveals that the $d_{x^2-y^2}$ orbital exhibits negligible sensitivity to E_{dc}^z , whereas the d_{z^2} orbital dominates the electronic density modulation. Specifically, the

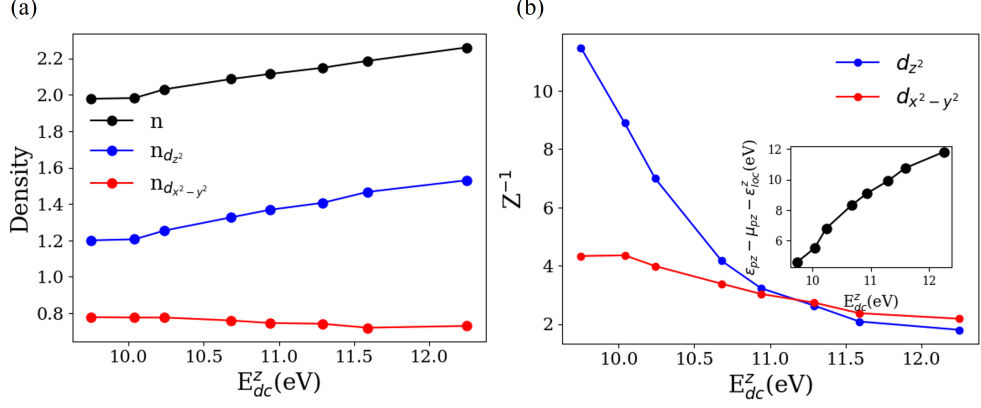


Fig. 3 (a) Electron densities as a function of E_{dc}^z . (b) Renormalization factor Z^{-1} for d_{z^2} and $d_{x^2-y^2}$ orbitals as a function of E_{dc}^z . Inset show the quantity $\epsilon_{pz} - \mu_{pz} - \epsilon_{loc}^z$ as a function of E_{dc}^z , which is proportional to the charge-transfer energy E_{dp} and can be regarded as a reference.

monotonic increase of $n_{d_{z^2}}$ with E_{dc}^z originates from the growth of the d_{z^2} bonding-state peak near -1 eV as E_{dc}^z increase shown in Fig. 2. In contrast, DOS of the $d_{x^2-y^2}$ orbital below the Fermi level remains largely unaffected by E_{dc}^z , indicating its weak role in this energy-dependent charge redistribution.

The correlation effect can be quantified using the quasiparticle mass renormalization factor $\frac{m^*}{m} = Z^{-1} = 1 - \frac{\partial \text{Im}\Sigma(i\omega)}{\partial i\omega} \Big|_{i\omega \rightarrow 0}$ and we perform the renormalization factor varying with E_{dc}^z in Fig. 3(b). As the figure illustrated, the renormalization factors of both d_{z^2} and $d_{x^2-y^2}$ orbitals decrease monotonically with double counting values, with the d_{z^2} orbital exhibiting significantly higher sensitivity to double counting adjustments compared to the $d_{x^2-y^2}$ orbital. Experimental measurements of the d_{z^2} orbital's renormalization factor yield a value of approximately 5, corresponding to $E_{dc}^z \sim 10.5$ eV in the plotted data. The inset in Fig. 3(b) shows the quantity $\epsilon_{pz} - \mu_{pz} - \epsilon_{loc}^z$ as a function of E_{dc}^z , which is proportional to the charge-transfer energy E_{dp} . From a theoretical perspective, a lower E_{dp} value enhances interlayer charge transfer phenomena, which manifests computationally as an amplified interlayer term in the Matsubara self-energy.

Fig. 4 investigates the interplay between E_{dc} and interlayer charge transfer dynamics by plotting the Matsubara self-energy interlayer term as a function of (E_{dc}^z, E_{dc}^x) . Notably, data points sharing identical self-energy values in panels (a) and (b) correspond to the same parameter set. The analysis reveals a similar evolution of the self-energy with respect to both double-counting corrections of d_{z^2} and $d_{x^2-y^2}$ orbitals. Specifically, in Fig. 4(a)(Fig. 4(b)) the interlayer self-energy exhibits a sharp increase at $E_{dc}^z \sim 10.1$ eV ($E_{dc}^x \sim 8.3$ eV), peaks around $E_{dc}^z \sim 10.2$ eV ($E_{dc}^x \sim 8.4$ eV), and subsequently decays with further elevation of E_{dc} . This non-monotonic behavior deviates significantly from the trend observed in the inset of Fig. 3(b). To reconcile this discrepancy, we analyze DOS evolution in Fig. 2(f)-(h). The emergence of metallic states in Fig. 2(g)-(h) disrupts the prerequisite for interlayer charge transfer mediated by

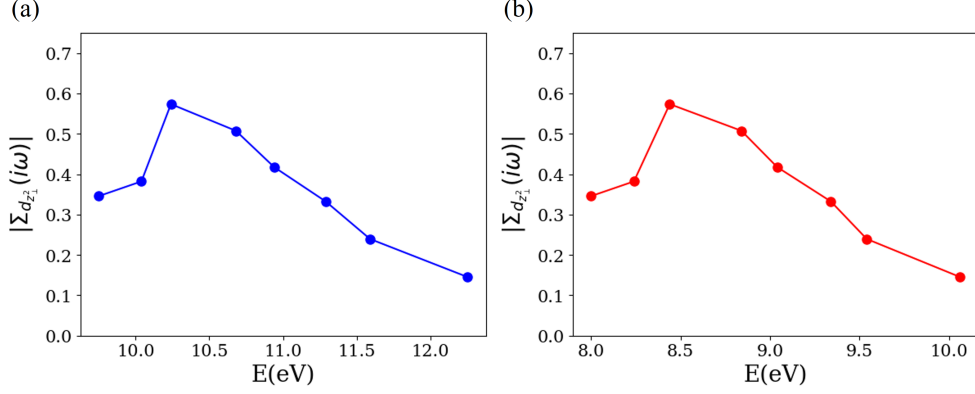


Fig. 4 (a),(b) show the interlayer term in d_{z^2} of Matsubara self-energy varying with double counting values in (E_{dc}^z, E_{dc}^x) . Data points sharing identical self-energy values in panels (a) and (b) correspond to the same parameter set.

oxygen bridges. This breakdown in the charge-transfer pathway explains the divergence between the $\epsilon_{pz} - \mu_{pz} - \epsilon_{loc}^z$ vs E_{dc}^z curve and the self-energy interlayer term's dependence on E_{dc} .

To validate against computational results, we evaluated two widely-used double counting estimation methods: (i) FLL form introduced in Ref.[7], which has the simple form $E_{dc} = U(n_0 - \frac{1}{2}) - \frac{J_H}{2}(n_0 - 1) = -14.8$, and $n_0 = 2.44$ stands for the occupancy in e_g orbital in no-interacting limit, (ii) Held formulas introduced in Ref.[12] with the form $E_{dc} = \frac{1}{3}(U + U - 2J_H + U - 3J_H)(n_0 - \frac{1}{2}) = -12.29$. Due to the neglect of energy-level splitting caused by apical oxygen in e_g orbitals, none of these approximations provided distinct double counting values for the d_{z^2} and $d_{x^2-y^2}$ orbitals. The Fermi surfaces calculated by the aforementioned methodology exhibit significant deviations from experimental measurements due to this inherent limitation.

4 Conclusion

This study employs CDMFT to investigate the double-counting correction effects on the correlated electronic structure of $\text{La}_3\text{Ni}_2\text{O}_7$ under ambient pressure, with fixed Fermi surface and adjusted parameters $E_{dc}^z, E_{dc}^x, \mu_{pz}$ at $\beta = 25$. Our calculations reveal a distinct orbital-selective DOS change: the d_{z^2} orbital undergoes the significant variation of DOS near the Fermi level with increasing E_{dc}^z , while the $d_{x^2-y^2}$ orbital remains essentially unchanged across the entire E_{dc}^z range. Orbital-resolved electron density calculations reveal different dependence of d_{z^2} and $d_{x^2-y^2}$ orbitals on double-counting corrections, with the d_{z^2} orbital exhibiting significantly stronger sensitivity to double-counting adjustments compared to its $d_{x^2-y^2}$ counterpart. Analysis of renormalization factors shows the monotonic dependence on double counting in both d_{z^2} and $d_{x^2-y^2}$ orbitals, and it also identifies an optimal E_{dc}^z window (10.2-10.5eV) where $Z_{d_{z^2}}^{-1} = 5-7$

aligns with experimental values, whereas the overestimated $Z_{d_{x^2-y^2}}^{-1} = 3$ (vs. experimental $Z^{-1} \sim 2$) likely stems from the Hubbard $U=8\text{eV}$ in our model. The analysis of Matsubara self energy reveals a similar evolution with respect to both d_{z^2} - and $d_{x^2-y^2}$ -orbital double-counting corrections, and it has a nonlinear deviation from theoretical predictions, which we attribute to the metallization of oxygen-bridged pathways that decouples charge transfer efficiency from E_{dp} magnitude. These findings highlight the critical role of double counting parameter selection in modeling nickelate superconductors and provide a computational framework for future studies of layered correlated materials.

5 Data availability

The data are available via contacting the corresponding author upon request

6 Acknowledgements

See funding support.

7 Competing interest

No potential conflict of interest was reported by the authors.

8 Funding

This project was supported by NSFC-92165204, NSFC-12494591, NSFC-92565303, NKRDPC-2022YFA1402802, Guangdong Provincial Key Laboratory of Magnetoelectric Physics and Devices (2022B1212010008), Research Center for Magnetoelectric Physics of Guangdong Province (2024B0303390001), Guangdong Provincial Quantum Science Strategic Initiative (GDZX2401010), and National Supercomputer Center in Guangzhou.

9 Authors' contributions

9.1 Authors and Affiliations

Guangdong Provincial Key Laboratory of Magnetoelectric Physics and Devices, State Key Laboratory of Optoelectronic Materials and Technologies, Center for Neutron Science and Technology, School of Physics, Sun Yat-sen University, Guangzhou, Guangdong 510275, China

Zhong-Yi Xie, Zhihui Luo, Wéi Wú, and Dao-Xin Yao

9.2 Contributions

Dao-Xin Yao and Wéi Wú conceived and designed the project. Zhong-Yi Xie wrote the code. Zhong-Yi Xie and Zhihui Luo performed the theoretical calculations and corresponding analysis under the supervision of Dao-Xin Yao and Wéi Wú. Dao-Xin

Yao supervised the project and proposed the relevant physical picture. All authors contributed to the interpretation of the results and wrote the paper.

9.3 Corresponding author

Correspondence to Dao-Xin Yao

References

- [1] Park H, Martin I. DFT + DMFT study of the magnetic susceptibility and the correlated electronic structure in transition-metal intercalated NbS₂. Phys. Rev. B 109, 085110 (2024)
- [2] James A D N, Aichhorn M, Laverock J. Composition-driven Mott transition within SrTi_{1-x}V_xO₃. <https://arxiv.org/abs/2309.00479> (2023)
- [3] Katanin A A. Magnetic properties of a half metal from the paramagnetic phase: DFT+DMFT study of exchange interactions in CrO₂. Phys. Rev. B 110, 155115 (2024)
- [4] Zaanen J, Sawatzky G A, Allen J W. Band gaps and electronic structure of transition-metal compounds. Phys. Rev. Lett. 55, 418 (1985)
- [5] Anisimov V I, Zaanen J, Andersen O K. Band theory and Mott insulators: Hubbard U instead of Stoner I. Phys. Rev. B 44, 943 (1991)
- [6] Anisimov V I, Solovyev I V, Korotin M A, et al. Density-functional theory and NiO photoemission spectra. Phys. Rev. B 48, 16929 (1993)
- [7] Czyzyk M T, Sawatzky G A. Local-density functional and on-site correlations: The electronic structure of La₂CuO₄ and LaCuO₃. Phys. Rev. B 49, 14211 (1994)
- [8] Sun H, Huo M, Hu X, et al. Signatures of superconductivity near 80 K in a nickelate under high pressure. Nature 621, 493 (2023).
- [9] Luo Z, Lv B, Wang M, et al. High-TC superconductivity in La₃Ni₂O₇ based on the bilayer two-orbital t-J model. npj Quantum Mater. 9, 61 (2024)
- [10] Wu W, Luo Z, Yao D, et al. Superexchange and charge transfer in the nickelate superconductor La₃Ni₂O₇ under pressure. Sci. China Phys. Mech. Astron. 67, 117402 (2024)
- [11] Yang J, Sun H, Hu X, et al. Orbital-dependent electron correlation in double-layer nickelate La₃Ni₂O₇. Nat. Commun. 15, 4373 (2024)
- [12] Held K. Electronic structure calculations using dynamical mean field theory. Advances in Physics, 56(6), 829-926 (2007)
- [13] Kresse G, Hafner J. Ab initio molecular dynamics for liquid metals. Phys. Rev. B 47, 558 (1993)
- [14] Kresse G, Furthmüller J. Efficient iterative schemes for ab initio total-energy calculations using a plane-wave basis set. Phys. Rev. B 54, 11169 (1996)
- [15] Blochl P E. Projector augmented-wave method. Phys. Rev. B 50, 17953 (1994)
- [16] Perdew J P, Burke K, Ernzerhof M. Generalized gradient approximation made simple. Phys. Rev. Lett. 78, 1396 (1997)
- [17] Luo Z, Hu X, Wang M, et al. Bilayer Two-Orbital Model of La₃Ni₂O₇ under Pressure. Phys. Rev. Lett. 131, 126001 (2023)
- [18] Georges A, Kotliar G. Hubbard model in infinite dimensions. Phys. Rev. B 45, 6479 (1992)

- [19] Georges A, Kotliar G, Krauth W, et al. Dynamical mean-field theory of strongly correlated fermion systems and the limit of infinite dimensions. *Rev. Mod. Phys.* 68, 13 (1996)
- [20] Kotliar G, Savrasov S Y, Haule K, et al. Electronic structure calculations with dynamical mean-field theory. *Rev. Mod. Phys.* 78, 865 (2006)
- [21] Maier T, Jarrell M, Pruschke T, et al. Quantum cluster theories. *Rev. Mod.Phys.* 77, 1027 (2005)
- [22] Yang J J, Yao D X, Wu H Q. Correlation effects in a simplified bilayer two-orbital Hubbard model at half filling. *Phys. Rev. B* 110, 235155 (2024)
- [23] She J H, Wang J X, He R Q, et al. Absence of two-orbital superconductivity in cuprate family: A DFT+DMFT perspective. *arXiv.2509.08823* (2025)
- [24] Parcollet O, Ferrero M, Ayrat T, et al. TRIQS: A toolbox for research on interacting quantum systems. *Computer Physics Communications* 196, 398 415 (2015)
- [25] Seth P, Krivenko I, Ferrero M, et al. TRIQS/CTHYB: A continuous-time quantum Monte Carlo hybridisation expansion solver for quantum impurity problems. *Computer Physics Communications* 200, 274 284 (2016)
- [26] Pourovskii L V, Amadon B, Biermann S, et al. Self-consistency over the charge density in dynamical mean-field theory: A linear muffin-tin implementation and some physical implications. *Phys. Rev. B* 76, 235101 (2007)